

Histone deacetylase inhibitor OBP-801 and amrubicin synergistically inhibit the growth of squamous cell lung carcinoma by inducing mitochondrial ASK1-dependent apoptosis

YUSUKE CHIHARA^{1,2}, YOSUKE IIZUMI¹, MANO HORINAKA¹,
MOTOKI WATANABE¹, WAKANA GOI¹, MIE MORITA¹, EMI NISHIMOTO¹, YOSHIHIRO SOWA¹,
TADAAKI YAMADA², KOICHI TAKAYAMA² and TOSHIYUKI SAKAI¹

Departments of ¹Molecular-Targeting Cancer Prevention and ²Pulmonary Medicine,
Graduate School of Medical Science, Kyoto Prefectural University of Medicine, Kyoto 602-8566, Japan

Received July 20, 2019; Accepted December 3, 2019

DOI: 10.3892/ijo.2020.4969

Abstract. Squamous cell lung carcinoma (SQCLC) is an aggressive type of lung cancer. In contrast with the marked advances that have been achieved in the treatment of lung adenocarcinoma, there are currently no effective targeted therapies for SQCLC, for with cytotoxic drugs are still the main treatment strategy. Therefore, the present study aimed to develop novel combination therapies for SQCLC. The results demonstrated that a combined treatment with the potent histone deacetylase (HDAC) inhibitor OBP-801 and the third-generation anthracycline amrubicin synergistically inhibited the viability of SQCLC cell lines by inducing apoptosis signal-regulating kinase 1 (ASK1)-dependent, as well as JNK- and p38 mitogen-activated protein kinase (MAPK)-independent apoptosis. OBP-801 treatment strongly induced the protein expression levels of thioredoxin-interacting protein (TXNIP), and amrubicin treatment increased the levels of intracellular reactive oxygen species (ROS), which suggested that this combination oxidized and dissociated thioredoxin 2 (Trx2) from mitochondrial ASK1 and activated ASK1. Moreover, mouse xenograft experiments using human H520 SQCLC cells revealed that the co-treatment potently suppressed tumor growth *in vivo*. These results suggested that a combined treatment with OBP-801 and amrubicin may have potential as a therapeutic strategy for SQCLC.

Introduction

Lung cancer is a leading cause of cancer morbidity (11.6% in 2018) and cancer-related mortality (18.4% in 2018) worldwide (1); it induces a number of symptoms, such as cough and dyspnea, and occlusion and cavitation by tumors sometimes cause severe lung infections (2-5). Non-small cell lung carcinoma (NSCLC) accounts for ~85% of all cases of lung cancer, of which 20-30% are squamous cell lung carcinoma (SQCLC) (6). Although molecular targeted therapies have markedly prolonged the survival of patients with lung adenocarcinoma, there are currently no developed effective targeted therapies for SQCLC. Amplification of the fibroblast growth factor receptor 1 (*FGFR1*) gene is one of the most common oncogenic alternations in SQCLC. Although clinical trials on FGFR inhibitors for patients with *FGFR*-amplified SQCLC have been conducted, the overall response rates were only 8-11% (7,8). Therefore, the prognosis of patients with SQCLC remains poor and treatment options are limited, and further research on the development of novel effective therapies for SQCLC is needed.

The third-generation anthracycline amrubicin is a potent topoisomerase II inhibitor that is approved in Japan for the treatment of NSCLC and small cell lung carcinoma (SCLC). A randomized phase III study comparing amrubicin and docetaxel (DOC) treatment in patients with previously treated NSCLC was conducted, and the median progression-free survival was 3.6 months in the amrubicin group and 3.0 months in the DOC group (P=0.54) (9). Although this study was unable to demonstrate the superiority of amrubicin over DOC, amrubicin is still regarded as one of the treatment options for patients with previously treated NSCLC in Japan.

Histone deacetylases (HDACs) are enzymes that serve important roles in changing epigenetic conditions and regulating gene expression (10). The strong expression of HDACs has been reported in various cancers, including lung cancer, and HDAC inhibitors block the proliferation of various lung cancer cell lines (11-13). Although HDAC inhibition is expected to become a new prospective treatment for lung cancer, HDAC inhibitor monotherapies for patients with

Correspondence to: Dr Yosuke Iizumi, Department of Molecular-Targeting Cancer Prevention, Graduate School of Medical Science, Kyoto Prefectural University of Medicine, Kawaramachi-Hirokoji, Kamigyo-ku, Kyoto 602-8566, Japan
E-mail: yiizumi@koto.kpu-m.ac.jp

Key words: reactive oxygen species, thioredoxin-interacting protein, thioredoxin, JNK, p38 mitogen-activated protein kinase, anthracycline

NSCLC have failed to exhibit clinical efficacy in clinical trials (14,15). Therefore, several clinical trials on combination therapies with HDAC inhibitors and cytotoxic drugs have been conducted, but failed to demonstrate the efficacy and safety of these therapies (16,17). OBP-801, also known as YM753, is one of the most potent HDAC inhibitors that was discovered in our previous study by screening for cyclin-dependent kinase inhibitor p21^{WAF1/Cip1}-inducing agents (18). OBP-801 is currently in a clinical trial in the USA and is a promising HDAC inhibitor.

To develop a novel combination therapy with the HDAC inhibitor OBP-801 against SQCLC, cytotoxic drugs approved for the treatment of SQCLC were screened and it was revealed that co-treatment with OBP-801 and amrubicin synergistically inhibited the viability of human SQCLC cells by inducing apoptosis. Moreover, the combined treatment was effective in H520 SQCLC xenograft model mice. The combined treatment with OBP-801 and amrubicin may have potential as a treatment option for patients with SQCLC.

Materials and methods

Reagents. Amrubicin was purchased from APEX BIO Technology LLC, and OBP-801 was from Oncolys BioPharma Inc. Doxorubicin hydrochloride was purchased from FUJIFILM Wako Pure Chemical Corporation. Selonsertib, SB203580 and SP600125 were purchased from Selleck Chemicals. The pan-caspase inhibitor Z-VAD-FMK was purchased from R&D Systems, Inc. These agents were dissolved in DMSO for *in vitro* experiments. N-acetyl-L-cysteine (NAC) was purchased from Nacalai Tesque, Inc.

Lung cancer cell lines and cell cultures. The human SQCLC cell lines Calu-1 and H520, and the lung adenocarcinoma cell line A549 were obtained from the American Type Culture Collection. Calu-1 and A549 cells were cultured in DMEM (Nissui Pharmaceutical Co., Ltd.) supplemented with 10% FBS (Sigma-Aldrich; Merck KGaA), 4 mM glutamine, 50 U/ml penicillin and 100 µg/ml streptomycin at 37°C in 5% CO₂. H520 cells were cultured in RPMI-1640 medium with 10% FBS, 2 mM glutamine, 50 U/ml penicillin and 100 µg/ml streptomycin at 37°C in 5% CO₂.

Treatments with agents. For cell viability assay, Calu-1 (1x10³ cells/well), A549 (1x10³ cells/well) and H520 cells (2x10³ cells/well) in a 96-well plate were treated with various concentrations of OBP-801 or amrubicin, or OBP-801 (Calu-1, 2.75 nM; A549, 2.5 nM; H520, 4.5 nM) with or without amrubicin (Calu-1, 2 µM; A549, 400 nM; H520, 4 µM) at 37°C for 72 h. For quantification of apoptosis, Calu-1 (5x10⁴ cells/well), A549 (2x10⁴ cells/well) and H520 cells (1.5x10⁵ cells/well) in a 6-well plate were treated with OBP-801 (Calu-1, 2.75 nM; A549, 2.5 nM; H520, 4.5 nM) with or without amrubicin (Calu-1, 2 µM; A549, 400 nM; H520, 4 µM) in the presence or absence of 5 mM NAC or 20 µM Z-VAD-FMK at 37°C for 72 h. In addition, Calu-1 cells (5x10⁴ cells/well in a 6-well plate) were also treated with 2.75 nM OBP-801 with or without 2 µM amrubicin in the presence or absence of 50 µM selonsertib, 50 µM SB203580 or 50 µM SP600125 at 37°C for 72 h, after which apoptosis was analyzed. For western blot analysis,

Calu-1 cells (3x10⁵ cells/10-cm dish) were treated with 2.75 nM OBP-801 with or without 2 µM amrubicin at 37°C for 72 h. For measuring intracellular ROS, Calu-1 cells (5x10⁴ cells/well in a 6-well plate) were treated with 2.75 nM OBP-801 with or without 2 µM amrubicin at 37°C for 48 h.

Cell viability assay. Following the various treatments of Calu-1, A549 and H520 cells, viability was evaluated using Cell Counting Kit-8 (CCK-8; Dojindo Molecular Technologies, Inc.), as previously described (19).

Quantification of apoptosis. Treated Calu-1, A549 and H520 cells were stained for 1 min at room temperature with 50 µg/ml propidium iodide. The cells were analyzed using a BD FACSCalibur (Becton, Dickinson and Company), and the degree of apoptosis was determined by quantifying the sub-G1 population (the left side of the G1 peak) using BD CellQuest Pro software (version 6.0; Becton, Dickinson and Company), as previously described (19).

Western blot analysis. Treated Calu-1 cells were lysed with RIPA buffer (50 mM Tris-HCl, pH 8.0; 150 mM NaCl; 1% NP-40; 0.5% deoxycholic acid; 0.1% SDS; 1 mM dithiothreitol; and 0.5 mM phenylmethylsulfonyl fluoride) for 30 min at 4°C, and western blotting was performed as previously described (19). Total protein concentration was measured using Bio-Rad Protein Assay Dye Reagent Concentrate (Bio-Rad Laboratories, Inc.). A total of 5–20 µg of protein was separated by 12% SDS-PAGE. The proteins were subsequently transferred to Immobilon-P membranes (Millipore; Merck KGaA), which were then blocked in Tris-buffered saline containing 5% skim milk for 1 h at room temperature. The membranes were incubated with the following primary antibodies for 1 h at room temperature: Anti-thioredoxin-interacting protein (TXNIP; 1:500; cat. no. ab188865; Abcam), anti-thioredoxin 2 (Trx2; 1:500; cat. no. sc-133201; Santa Cruz Biotechnology, Inc.), anti-cleaved poly (ADP-ribose) polymerase (Asp214) (PARP; 1:1,000; cat. no. 5625; Cell Signaling Technology, Inc.) and anti-β-actin (1:2,000; cat. no. A5441; Sigma-Aldrich; Merck KGaA). Membranes were then incubated with the following secondary antibodies for 1 h at room temperature: Horseradish peroxidase (HRP)-conjugated sheep anti-mouse IgG (1:2,000; cat. no. NA931; GE Healthcare) or HRP-conjugated donkey anti-rabbit IgG (1:2,000; cat. no. NA934; GE Healthcare). Proteins were visualized with Chemi-Lumi One L (Nacalai Tesque) or Immobilon Western Chemiluminescent HRP Substrate (Millipore; Merck KGaA) and detected on BioMax XAR film (Carestream Health, Inc.).

Measurement of intercellular ROS. Treated Calu-1 cells were incubated with 5 µM CellROX Deep Red Reagent (Thermo Fisher Scientific, Inc.) for 30 min at 37°C. Fluorescence signals were measured in the FL-4 channel by FACSCalibur and BD CellQuest Pro software (version 6.0).

siRNA transfection. The following siRNAs targeting Trx2 were purchased from Thermo Fisher Scientific, Inc.; only sense strands are shown: siTrx2#1, 5'-CCCGGACAAUACACACGAGGAU-3'; siTrx2#2, 5'-CCACACAGACCUCCCAUUGAGUAU-3'; and siTrx2#3, 5'-GCCUCCUG

AAGAAGCUGAUUGGCU-3'; and a negative control siRNA (cat. no. 12935-113). Calu-1 cells (3×10^4 cells/well in a 6-well plate) were transfected with each siRNA (30 pmol) at 37°C using Lipofectamine® RNAiMAX (Thermo Fisher Scientific, Inc.), according to the manufacturer's protocol. After 5 h, the medium was replaced. A total of 48 h post-transfection, the cells were lysed with RIPA buffer, and the knockdown efficiency of each siRNA was confirmed by western blotting. At 120 h post-transfection, the proportion of apoptotic cells (the sub-G1 population) was analyzed using FACSCalibur and BD CellQuest Pro software (version 6.0) aforementioned.

Mouse xenograft model. Female BALB/c *nu/nu* mice (n=20; age, 5 weeks; weight, 16.85-21.78 g) were purchased from Charles River Laboratories, Inc. The mice were housed in cages at 24±2°C and 45±5% humidity under pathogen-free conditions and fed CLEA rodent diet CE-2 commercial pellets (CLEA Japan, Inc.) and tap water *ad libitum*. All experiments were performed in accordance with the institutional animal care and use committee guidelines, and the present study was approved by the Committee for Animal Research of Kyoto Prefectural University of Medicine (permission no. M29-576). A total of 4×10^6 untreated H520 cells mixed with Matrigel (BD Biosciences) were injected subcutaneously into the right flank of mice. Tumor volumes were calculated using the following formula: $\frac{1}{2} \times \text{length} \times \text{width}^2$. When tumor volumes reached 40 mm³ on average on day 13, mice were randomized into four groups (n=5 mice per group) and treatments were initiated. OBP-801 was dissolved in saline containing 20% hydroxypropyl-β-cyclodextrin, and mice were injected through the tail vein once a week (on days 15, 22, 29 and 36) with diluent or OBP-801 (10 mg/kg). Amrubicin hydrochloride (Nippon Kayaku Co., Ltd.) was dissolved in saline, and mice were injected through the tail vein only once (on day 14) with diluent or amrubicin (25 mg/kg). The concentrations of OBP-801 and amrubicin used were based on the results of pre-experiments (data not shown). Tumor sizes were measured twice per week, and the experiment was finished on day 72. The humane endpoints established for this study were mice exhibiting abnormalities such as a sudden weight loss of ≥20%, or tumor size in a single mouse exceeds 2,000 mm³. The mice were euthanized by intraperitoneal injection of 200 mg/kg pentobarbital.

Statistical analysis. Data are expressed as the mean ± SD of three measurements. Statistical analyses were performed using ANOVA followed by Bonferroni's post hoc test. Combination index (CI) values were calculated using CalcuSyn software (version 2.0; Biosoft, Cambridge, UK); a combination was judged to be synergistic when CI <1.0. P<0.05 was considered to indicate a statistically significant difference.

Results

Combined OBP-801 and amrubicin treatment synergistically inhibits human lung cancer cell line viability. To evaluate the effects of combined treatments with the potent HDAC inhibitor OBP-801, the effects of OBP-801 or amrubicin alone on the viability of human SQCLC Calu-1 cells were examined. Each agent inhibited the viability of Calu-1 cells

in a dose-dependent manner (Fig. 1A). The effects of several combinations were then analyzed by combining OBP-801 and amrubicin at various concentrations near the IC₅₀; the combined treatment with OBP-801 and amrubicin more strongly inhibited the viability of Calu-1 cells than the treatment with each agent alone (Fig. 1B). Based on the viability inhibition curves concerning human SQCLC H520 cells (Fig. S1A) and human lung adenocarcinoma A549 cells (Fig. S1B), the effects of several combinations were also examined by combining OBP-801 and amrubicin at various concentrations near the IC₅₀, and similar results were obtained using H520 and A549 cells (Fig. 1C). Moreover, OBP-801 and another anthracycline, doxorubicin, also coordinately inhibited the viability of Calu-1 cells (Fig. S2). The CI value for the combination of OBP-801 and amrubicin against Calu-1 cells was markedly <1.0 (Fig. 1D), which indicated synergistic inhibition against the viability of Calu-1 cells.

Co-treatment with OBP-801 and amrubicin induces caspase-dependent and ROS-dependent apoptosis in lung cancer cells. To clarify the mechanisms underlying synergistic viability inhibition by the combination of OBP-801 and amrubicin, the effects of this combination on Calu-1 cells was examined using flow cytometric analysis of apoptotic cell proportions at Sub-G1. OBP-801 or amrubicin alone slightly induced apoptosis compared with untreated cells, but the differences were not significant, whereas the co-treatment with OBP-801 and amrubicin significantly increased apoptosis in Calu-1 cells compared with either treatment alone (Figs. 2A and S3). The combination notably induced the cleavage of the PARP protein (Fig. 2B). Since amrubicin and HDAC inhibitors are both known to increase the production of ROS (20-24), whether apoptosis was inhibited by the free radical scavenger NAC was examined. NAC was used at 5 mM according to our previous reports (25,26). NAC treatment inhibited apoptosis induced by the co-treatment with OBP-801 and amrubicin in Calu-1, H520 and A549 cells (Figs. 2C and S4-6). In addition, the pan-caspase inhibitor Z-VAD-FMK was used at 20 μM according to our previous reports (26,27); Z-VAD-FMK also significantly inhibited apoptosis in OBP-801 and amrubicin co-treated Calu-1, H520 and A549 cells (Figs. 2C and S4-6). These results suggested that the combined treatment with OBP-801 and amrubicin may induce ROS-mediated and caspase-dependent apoptosis in human lung cancer cell lines.

OBP-801 and amrubicin co-treatment induces apoptosis signal-regulating kinase 1 (ASK1)-dependent and JNK- and p38 mitogen-activated protein kinase (MAPK)-independent apoptosis. Since ROS is known to induce apoptosis by activating ASK1 and its downstream targets JNK and p38 MAPK (28), whether apoptosis induced by the co-treatment with OBP-801 and amrubicin depended on ASK1, JNK or p38 MAPK was investigated using their respective inhibitors. Based on previous reports (29,30), these inhibitors were used at the uniform concentration of 50 μM. The ASK1 inhibitor selonsertib significantly suppressed apoptosis induced by the combined treatment in Calu-1 cells (Figs. 3A and S7). However, neither the p38 MAPK inhibitor SB203580 nor JNK inhibitor SP600125 suppressed apoptosis induced by the combined

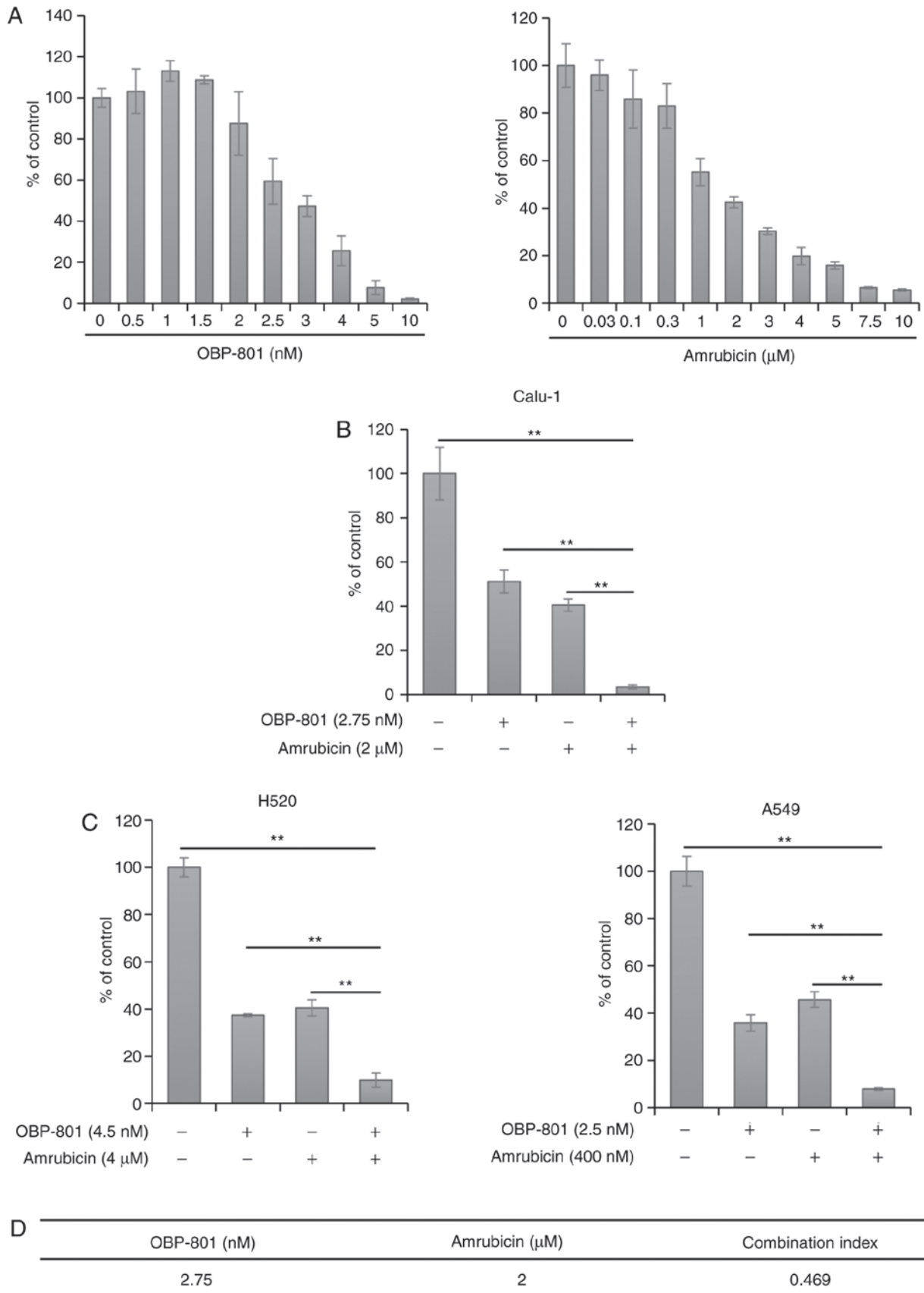


Figure 1. Combined treatment with OBP-801 and amrubicin synergistically inhibits the viability of human lung cancer cells. (A) Calu-1 human SQCLC cells were treated with various concentrations of OBP-801 or amrubicin. After 72 h, cell viability was assessed by the CCK-8 assay. (B) Calu-1 cells were treated with 2.75 nM OBP-801 with or without co-treatment with 2 μM amrubicin. After 72 h, cell viability was assessed by the CCK-8 assay. (C) H520 human SQCLC cells were treated with 4.5 nM OBP-801 with or without 4 μM amrubicin, and human lung adenocarcinoma A549 cells were treated with 2.5 nM OBP-801 with or without 400 nM amrubicin. After 72 h, cell viability was assessed by the CCK-8 assay. (D) The combination index value of the combination with OBP-801 and amrubicin against Calu-1 cells was calculated. Data are presented as the mean ± SD from three independent experiments; **P<0.01. CCK-8, Cell Counting Kit-8; SQCLC, squamous cell lung carcinoma.

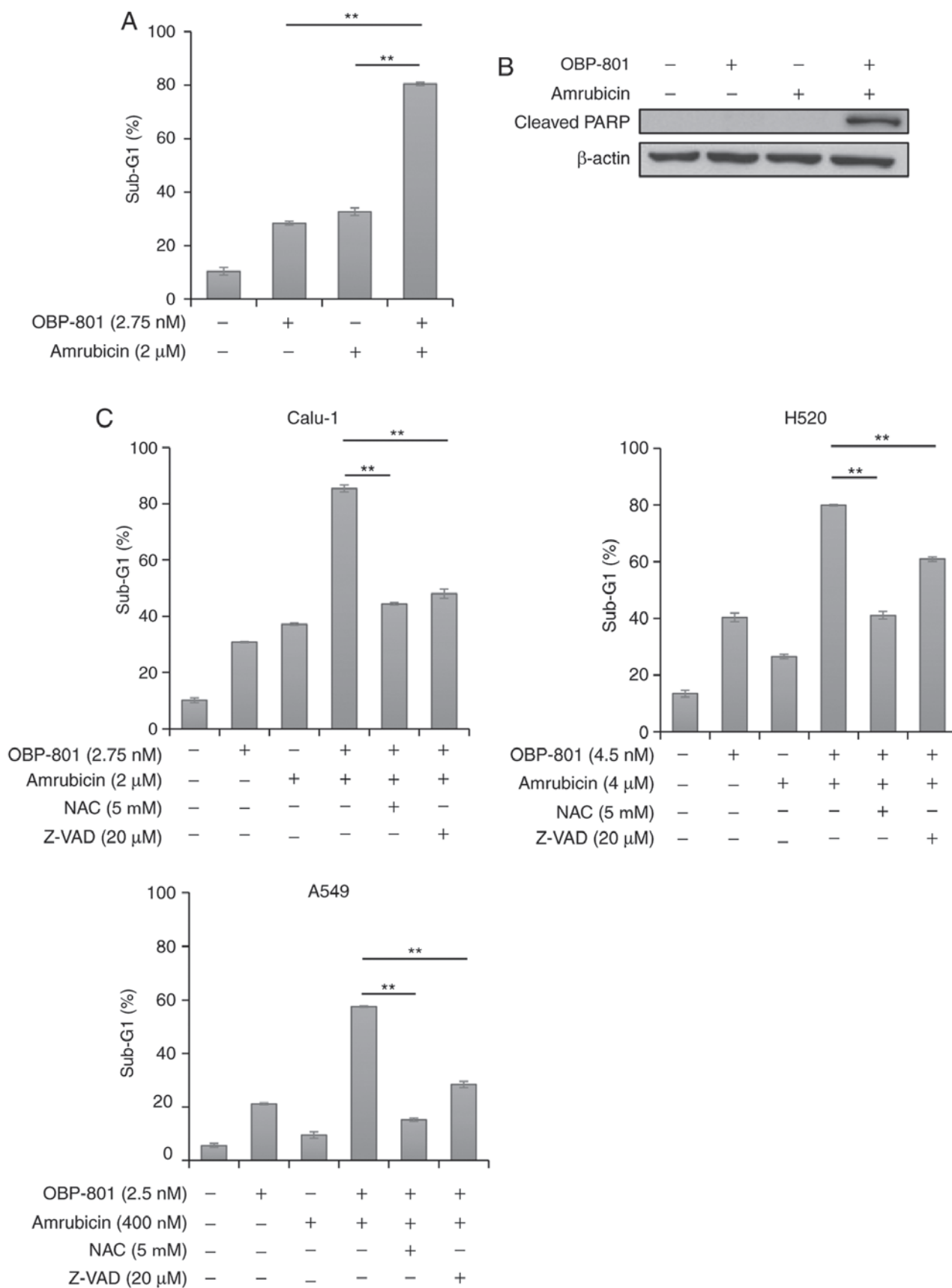


Figure 2. Combined treatment with OBP-801 and amrubicin induces caspase- and ROS-dependent apoptosis. (A) Calu-1 human squamous cell lung carcinoma cells were treated with 2.75 nM OBP-801 with or without 2 μM amrubicin for 72 h. The degree of apoptosis was assessed using flow cytometry to detect the percentage of cells at sub-G1. (B) Western blot analysis of cleaved PARP in Calu-1 cells treated with 2.75 nM OBP-801 with or without 2 μM amrubicin for 72 h. β-actin was used as a loading control. (C) Calu-1, H520 and A549 human lung cancer cells were treated with OBP-801 with or without amrubicin in the presence or absence of the free radical scavenger NAC or pan-caspase inhibitor Z-VAD-FMK for 72 h. The degree of apoptosis (sub-G1) was quantified using flow cytometry. Data are presented as the mean ± SD from three independent experiments; **P<0.01. NAC, N-acetyl-L-cysteine; PARP, poly (ADP-ribose) polymerase.

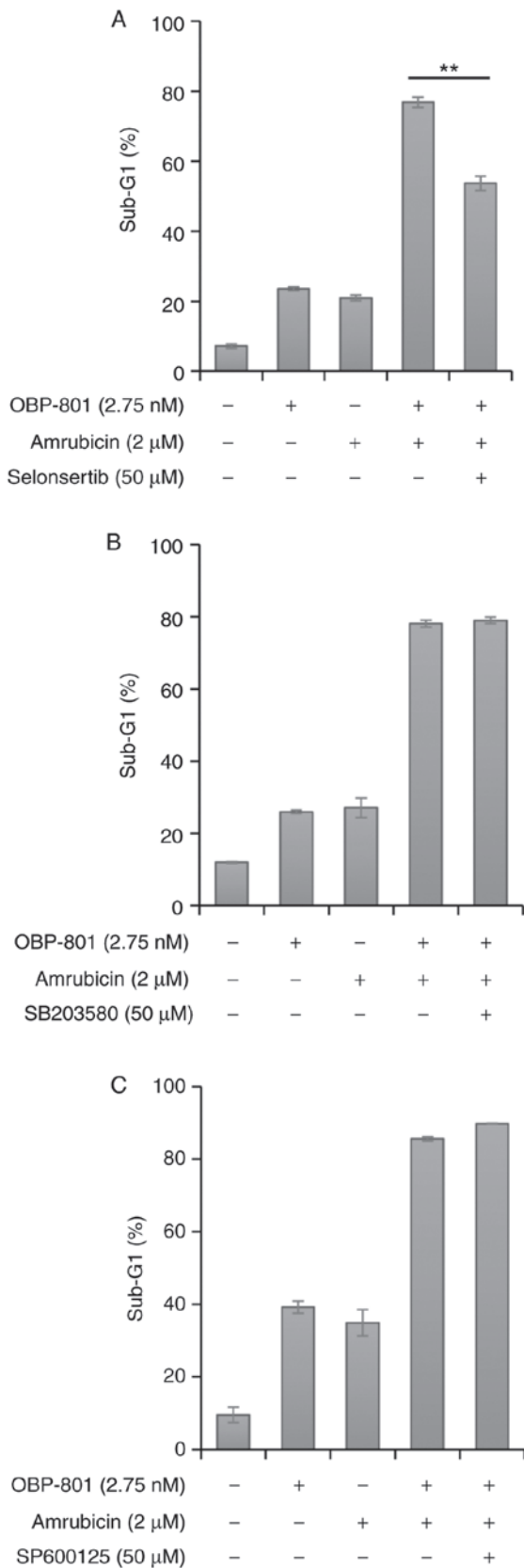


Figure 3. Combined treatment with OBP-801 and amrubicin induces ASK1-dependent and JNK- and p38 MAPK-independent apoptosis. (A-C) Calu-1 human squamous cell lung carcinoma cells were treated with 2.75 nM OBP-801 with or without 2 μM amrubicin in the presence or absence of (A) the ASK1 inhibitor selonsertib, (B) the p38 MAPK inhibitor SB203580, or (C) the JNK inhibitor SP600125 for 72 h. The degree of apoptosis (sub-G1) was assessed using flow cytometry. Data are presented as the mean ± SD from three independent experiments; **P<0.01. ASK1, apoptosis signal-regulating kinase 1; MAPK, mitogen-activated protein kinase.

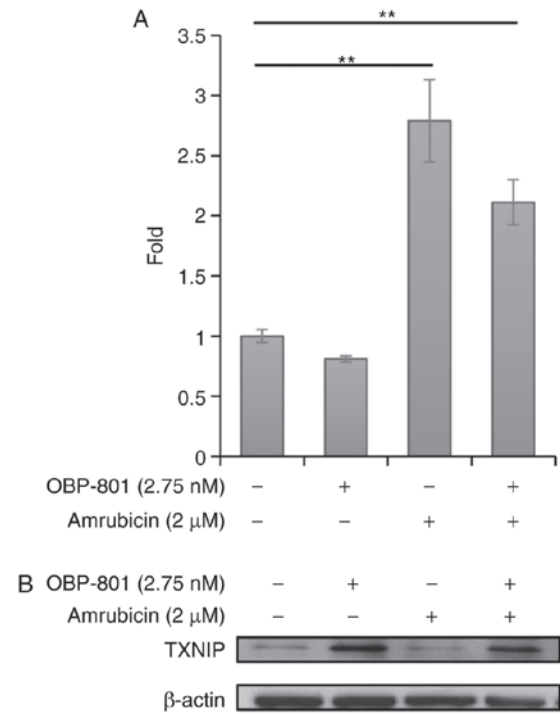


Figure 4. Amrubicin elevates ROS levels and OBP-801 increases TXNIP protein expression. (A) Calu-1 human squamous cell lung carcinoma cells were treated with 2.75 nM OBP-801 with or without 2 μM amrubicin. After 48 h, reactive oxygen species levels were analyzed using CellROX Deep Red Reagent. Data are presented as the mean ± SD from three independent experiments; **P<0.01. (B) Western blot analysis of the TXNIP protein expression in Calu-1 cells treated with 2.75 nM OBP-801 with or without 2 μM amrubicin for 72 h. β-actin was used as a loading control. TXNIP, thioredoxin-interacting protein.

treatment (Fig. 3B and C, respectively, and Figs. S8 and S9). These results indicated that apoptosis induced by the co-treatment with OBP-801 and amrubicin may be ASK1-dependent and JNK- and p38 MAPK-independent.

OBP-801 upregulates TXNIP protein expression and amrubicin increases intracellular ROS. ASK1 is inactivated by the binding of Trx, and ROS oxidize Trx, resulting in the dissociation of Trx from ASK1 and activation of ASK1 (31). A previous study reported that ASK1-dependent and JNK- and p38 MAPK-independent apoptosis was induced by mitochondrial ASK1, which was inactivated by Trx2 (32). Therefore, the relationship between the combined treatment with OBP-801 and amrubicin and the regulation of mitochondrial ASK1 was examined. Although OBP-801 alone slightly reduced intracellular ROS, which oxidizes Trx2, amrubicin alone or combination with OBP-801 increased it (Figs. 4A and S10). The TXNIP protein is also known to oxidize Trx2 in mitochondria and to dissociate Trx2 from mitochondrial ASK1 (32). We found that OBP-801 and its combination potentially induced TXNIP protein expression (Fig. 4B). These results suggested that ROS and TXNIP induced by amrubicin and OBP-801 might contribute to ASK1-dependent and JNK- and p38 MAPK-independent apoptosis.

Trx2 knockdown induces apoptosis in Calu-1 cells. To examine the significance of the disassociation of Trx2 from ASK1, Trx2 expression was knocked down in Calu-1 cells

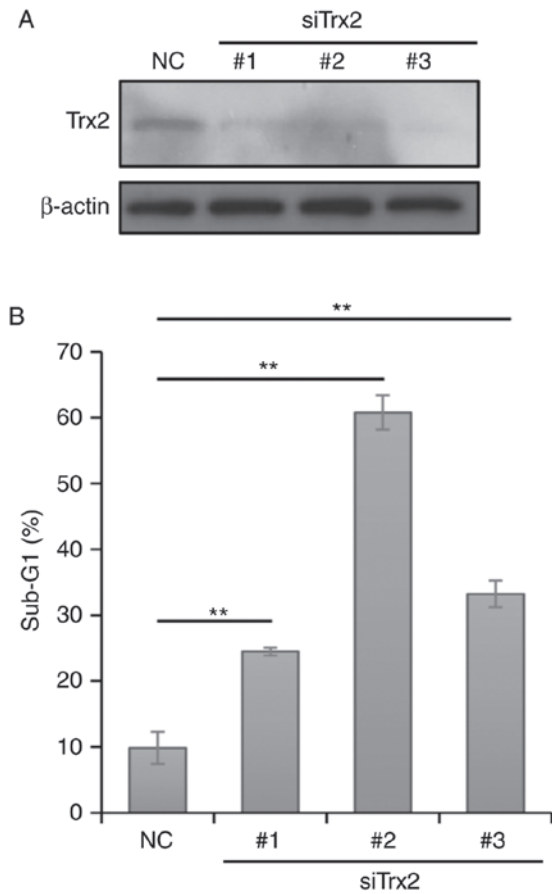


Figure 5. Depletion of Trx2 induces apoptosis in Calu-1 cells. (A) Western blot analysis of Trx2 protein expression was performed on Calu-1 human squamous cell lung carcinoma cells transfected with siTrx2#1, siTrx2#2, siTrx2#3 or an NC siRNA for 48 h. (B) Calu-1 cells were transfected with or without siTrx2 for 120 h, and the degree of apoptosis (sub-G1) was quantified using flow cytometry. Data are presented as the mean \pm SD from three independent experiments; * P <0.01. NC, negative control; si, small interfering RNA; Trx2, thioredoxin 2.

using siRNAs. siRNAs targeting Trx2 notably reduced Trx2 protein expression levels in transfected Calu-1 cells (Fig. 5A). The depletion of Trx2 significantly induced apoptosis in Calu-1 cells compared with control cells (Figs. 5B and S11), which suggested that inactivation of Trx2 induces apoptosis in SQCLC cells.

Combined treatment with OBP-801 and amrubicin inhibits tumor growth in vivo. Furthermore, the antitumor effects of the combined treatment with OBP-801 and amrubicin were examined in a mouse xenograft model. Since SQCLC H520 cells, but not Calu-1 cells, could be engrafted in BALB/c *nu/nu* mice, the SQCLC H520 xenograft model was used. The combined treatment significantly suppressed tumor growth compared with either treatment alone on day 40 (Fig. 6A). Although the treatment with amrubicin reduced the body weights of mice after the injection on day 18 as previously reported (33), body weights recovered within a few days, and no significant differences were observed between groups at the end of the study period (Fig. 6B). These results indicated that the combined treatment with OBP-801 and amrubicin effectively prevented the tumor growth of SQCLC *in vivo*.

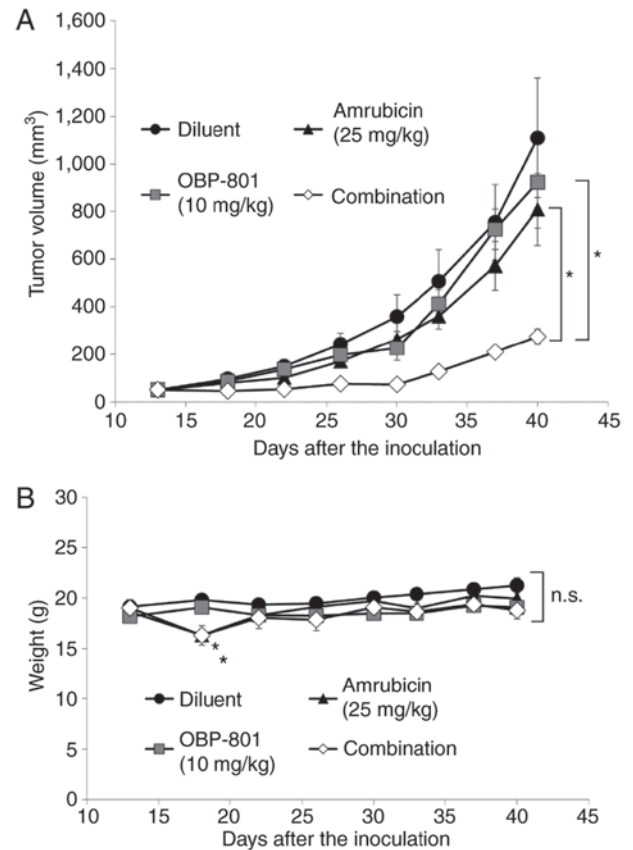


Figure 6. Combined treatment with OBP-801 and amrubicin suppresses tumor growth in a human squamous cell lung carcinoma xenograft model. Female BALB/c *nu/nu* mice were subcutaneously injected with untreated H520 cells. Mice were randomized on day 13 and subsequently intravenously treated with diluent, OBP-801 (10 mg/kg), amrubicin (25 mg/kg) or a combination of the two drugs. (A) Tumor growth curves of the four treatment groups. (B) Body weight curves of four treatment groups. Data are presented as the mean \pm SD; n=5 mice/group; * P <0.05. n.s., not significant.

Discussion

The treatment of advanced NSCLC has been markedly improved by the arrival of novel molecular targeted agents, such as gefitinib (34) and crizotinib (35), and immune checkpoint inhibitors, such as nivolumab (36) and pembrolizumab (37). However, no molecular targeted agents are currently approved for the treatment of SQCLC; thus, the development of novel effective treatment strategies for SQCLC is needed. In the present study, a combined treatment with the potent HDAC inhibitor OBP-801 and amrubicin was demonstrated to synergistically inhibit the viability of Calu-1 SQCLC cells by inducing mitochondrial ASK1-dependent apoptosis. Moreover, this combination strongly inhibited tumor growth in a SQCLC xenograft model. Limited information is currently available on combined treatments with HDAC inhibitors for SQCLC. Although the HDAC inhibitor ITF2357 was previously reported to enhance the cytotoxicity of pemetrexed against SQCLC cells (38), pemetrexed is not approved for the treatment of SQCLC. Since amrubicin is approved for the treatment of SQCLC in Japan, a combined treatment with OBP-801 and amrubicin may be a realistic combination therapy for SQCLC. Moreover, since this co-treatment was also effective against human lung adenocarcinoma A549 cells, it may have potential in the treatment of NSCLC.

Apoptosis induced by the combined treatment with OBP-801 and amrubicin was suppressed by the ROS scavenger NAC. Since HDAC inhibitors and amrubicin are known to increase intracellular ROS (20-24), it was speculated that OBP-801 and amrubicin both increased ROS, resulting in the strong induction of apoptosis. However, OBP-801 treatment alone did not induce ROS, and ROS levels in co-treatment cells did not exceed those by amrubicin alone. The mechanisms underlying the induced increase in apoptosis were examined, and it was demonstrated that OBP-801 strongly induced the TXNIP protein. Since the overexpression of TXNIP is known to enhance oxidative stress (39), OBP-801 might augment the anticancer effects of amrubicin, which has an ability to increase ROS, by inducing the TXNIP protein. The low dose of OBP-801 (2.75 nM), which did not increase ROS, enhanced the growth-inhibitory effect of amrubicin by strongly inducing TXNIP protein. In a mouse xenograft model, the low dose of OBP-801 (10 mg/kg), which could not suppress tumor growth alone, exhibited strong tumor growth inhibition in combination with amrubicin. Since enhanced expression of TXNIP protein is reported to augment oxidative damage (39), low doses of OBP-801 may potentiate the anticancer effects of the agents that exhibit cytotoxicity by inducing ROS.

Although some clinical trials on combination therapies with HDAC inhibitors and cytotoxic drugs against NSCLC have been conducted, safety was an important issue in these trials. A phase I trial of a combination with the HDAC inhibitor vorinostat and docetaxel was stopped due to excessive toxicity (16). In a randomized phase II trial evaluating the efficacy of vorinostat in combination with carboplatin and paclitaxel for advanced NSCLC, adverse events were more frequent than with a treatment involving carboplatin and paclitaxel (17). However, since the feasibility of the combination with the HDAC inhibitor valproate and doxorubicin was reported in a phase II trial on patients with malignant mesothelioma (40), combinations with HDAC inhibitors and anthracyclines may be relatively tolerable. Amrubicin is also reported to be more tolerable than doxorubicin concerning cardiotoxicity, which is a noteworthy adverse event associated with the use of anthracyclines (41,42). Therefore, the combined treatment with OBP-801 and amrubicin may be tolerable.

In conclusion, the present study demonstrated that a combined treatment with the potent HDAC inhibitor OBP-801 and amrubicin synergistically inhibited the viability of SQCLC cells by strongly inducing apoptosis. Furthermore, this combined treatment inhibited tumor growth in an *in vivo* xenograft model. To the best of our knowledge, the present study is the first to show the synergistic efficacy of a combined treatment with a HDAC inhibitor and anthracycline against Calu-1 SQCLC cells. Since combined treatments with HDAC inhibitors and anthracyclines may be tolerable, the combination of OBP-801 and amrubicin has potential in the treatment of SQCLC.

Acknowledgements

Not applicable.

Funding

This study was supported by a commercial research grant from Oncolys BioPharma, Inc. to TS.

Availability of data and materials

Not applicable.

Authors' contributions

YC, YI, YS, KT and TS conceived the study. YC, YI, MH and TY designed the experiments. YC, MW, WG, MM and EN performed the experiments. YC, YI, YS, TY, KT and TS wrote the manuscript and revised it critically. All authors have read and approved the final manuscript.

Ethics approval and consent to participate

The mouse xenograft study was performed in accordance with the institutional animal care and use committee guidelines and approved by the Committee for Animal Research of Kyoto Prefectural University of Medicine (Kyoto, Japan; permission no. M29-576).

Patient consent for publication

Not applicable.

Competing interests

The presented study was supported by a commercial research grant from Oncolys BioPharma, Inc. (Tokyo, Japan) to Dr Sakai. The remaining authors declare that they have no competing interests.

References

1. Bray F, Ferlay J, Soerjomataram I, Siegel RL, Torre LA and Jemal A: Global cancer statistics 2018: GLOBOCAN estimates of incidence and mortality worldwide for 36 cancers in 185 countries. *CA Cancer J Clin* 68: 394-424, 2018.
2. Ungureanu A, Zlatian O, Mitroi G, Drocas A, Țircă T, Calina D, Dehelean C, Docea AO, Izotov BN, Rakitskii VN, *et al*: Staphylococcus aureus colonisation in patients from a primary regional hospital. *Mol Med Rep* 16: 8771-8780, 2017.
3. Zlatian O, Balasoiu AT, Balasoiu M, Cristea O, Docea AO, Mitrut R, Spandidos DA, Tsatsakis AM, Bancescu G and Calina D: Antimicrobial resistance in bacterial pathogens among hospitalised patients with severe invasive infections. *Exp Ther Med* 16: 4499-4510, 2018.
4. Tanase A, Colita A, Ianosi G, Neagoe D, Branisteanu DE, Calina D, Docea AO, Tsatsakis A and Ianosi SL: Rare case of disseminated fusariosis in a young patient with graft vs. host disease following an allogeneic transplant. *Exp Ther Med* 12: 2078-2082, 2016.
5. Călina D, Roșu L, Roșu AF, Ianoși G, Ianoși S, Zlatian O, Mitruț R, Docea AO, Rogoveanu O, Mitruț P, *et al*: Etiological diagnosis and pharmacotherapeutic management of parapneumonic pleurisy. *Farmacia* 64: 946-952, 2016.
6. Travis WD: Pathology of lung cancer. *Clin Chest Med* 32: 669-692, 2011.
7. Paik PK, Shen R, Berger MF, Ferry D, Soria JC, Mathewson A, Rooney C, Smith NR, Cullberg M, Kilgour E, *et al*: A phase Ib open-label multicenter study of AZD4547 in patients with advanced squamous cell lung cancers. *Clin Cancer Res* 23: 5366-5373, 2017.
8. Nogova L, Sequist LV, Perez Garcia JM, Andre F, Delord JP, Hidalgo M, Schellens JH, Cassier PA, Camidge DR, Schuler M, *et al*: Evaluation of BGJ398, a fibroblast growth factor receptor 1-3 kinase inhibitor, in patients with advanced solid tumors harboring genetic alterations in fibroblast growth factor receptors: Results of a global phase I, dose-escalation and dose-expansion study. *J Clin Oncol* 35: 157-165, 2017.

9. Yoshioka H, Katakami N, Okamoto H, Iwamoto Y, Seto T, Takahashi T, Sunaga N, Kudoh S, Chikamori K, Harada M, *et al*: A randomized, open-label, phase III trial comparing amrubicin versus docetaxel in patients with previously treated non-small-cell lung cancer. *Ann Oncol* 28: 285-291, 2017.
10. Petta V, Gkizos I, Strimpakos A and Syrigos K: Histones and lung cancer: Are the histone deacetylases a promising therapeutic target? *Cancer Chemother Pharmacol* 72: 935-952, 2013.
11. Miyanaga A, Gemma A, Noro R, Kataoka K, Matsuda K, Nara M, Okano T, Seike M, Yoshimura A, Kawakami A, *et al*: Antitumor activity of histone deacetylase inhibitors in non-small cell lung cancer cells: Development of a molecular predictive model. *Mol Cancer Ther* 7: 1923-1930, 2008.
12. Sun L, He Q, Tsai C, Lei J, Chen J, Vienna Makcey L and Coy DH: HDAC inhibitors suppressed small cell lung cancer cell growth and enhanced the suppressive effects of receptor-targeting cytotoxins via upregulating somatostatin receptor II. *Am J Transl Res* 10: 545-553, 2018.
13. You BR and Park WH: Down-regulation of thioredoxin1 is involved in death of calu-6 lung cancer cells treated with suberoyl bishydroxamic acid. *J Cell Biochem* 117: 1250-1261, 2016.
14. Reid T, Valone F, Lipera W, Irwin D, Paroly W, Natale R, Sreedharan S, Keer H, Lum B, Scappaticci F and Bhatnagar A: Phase II trial of the histone deacetylase inhibitor pivaloyloxymethyl butyrate (Pivanex, AN-9) in advanced non-small cell lung cancer. *Lung Cancer* 45: 381-386, 2004.
15. Traynor AM, Dubey S, Eickhoff JC, Kolesar JM, Schell K, Huie MS, Groteluschen DL, Marcotte SM, Hallahan CM, Weeks HR, *et al*: Vorinostat (NSC# 701852) in patients with relapsed non-small cell lung cancer: A wisconsin oncology network phase II study. *J Thorac Oncol* 4: 522-526, 2009.
16. Schneider BJ, Kalemkerian GP, Bradley D, Smith DC, Egorin MJ, Daignault S, Dunn R and Hussain M: Phase I study of vorinostat (suberoylanilide hydroxamic acid, NSC 701852) in combination with docetaxel in patients with advanced and relapsed solid malignancies. *Invest New Drugs* 30: 249-257, 2012.
17. Ramalingam SS, Maitland ML, Frankel P, Argiris AE, Koczywas M, Gitlitz B, Thomas S, Espinoza-Delgado I, Vokes EE, Gandara DR and Belani CP: Carboplatin and paclitaxel in combination with either vorinostat or placebo for first-line therapy of advanced non-small-cell lung cancer. *J Clin Oncol* 28: 56-62, 2010.
18. Shindoh N, Mori M, Terada Y, Oda K, Amino N, Kita A, Taniguchi M, Sohda KY, Nagai K, Sowa Y, *et al*: YM753, a novel histone deacetylase inhibitor, exhibits antitumor activity with selective, sustained accumulation of acetylated histones in tumors in the WiDr xenograft model. *Int J Oncol* 32: 545-555, 2008.
19. Ono H, Iizumi Y, Goi W, Sowa Y, Taguchi T and Sakai T: Ribosomal protein S3 regulates XIAP expression independently of the NF- κ B pathway in breast cancer cells. *Oncol Rep* 38: 3205-3210, 2017.
20. Salvatorelli E, Menna P, Gonzalez Paz O, Surapaneni S, Aukerman SL, Chello M, Covino E, Sung V and Minotti G: Pharmacokinetic characterization of amrubicin cardiac safety in an ex vivo human myocardial strip model. II. Amrubicin shows metabolic advantages over doxorubicin and epirubicin. *J Pharmacol Exp Ther* 341: 474-483, 2012.
21. Petrucci LA, Dupéré-Richer D, Pettersson F, Retrouvey H, Skoulikas S and Miller WH Jr: Vorinostat induces reactive oxygen species and DNA damage in acute myeloid leukemia cells. *PLoS One* 6: e20987, 2011.
22. You BR and Park WH: Trichostatin A induces apoptotic cell death of HeLa cells in a Bcl-2 and oxidative stress-dependent manner. *Int J Oncol* 42: 359-366, 2013.
23. You BR, Kim SH and Park WH: Reactive oxygen species, glutathione, and thioredoxin influence suberoyl bishydroxamic acid-induced apoptosis in A549 lung cancer cells. *Tumour Biol* 36: 3429-3439, 2015.
24. Han BR, You BR and Park WH: Valproic acid inhibits the growth of HeLa cervical cancer cells via caspase-dependent apoptosis. *Oncol Rep* 30: 2999-3005, 2013.
25. Yoshioka T, Yogosawa S, Yamada T, Kitawaki J and Sakai T: Combination of a novel HDAC inhibitor OBP-801/YM753 and a PI3K inhibitor LY294002 synergistically induces apoptosis in human endometrial carcinoma cells due to increase of Bim with accumulation of ROS. *Gynecol Oncol* 129: 425-432, 2013.
26. Yamada T, Horinaka M, Shinnoh M, Yoshioka T, Miki T and Sakai T: A novel HDAC inhibitor OBP-801 and a PI3K inhibitor LY294002 synergistically induce apoptosis via the suppression of survivin and XIAP in renal cell carcinoma. *Int J Oncol* 43: 1080-1086, 2013.
27. Ono H, Sowa Y, Horinaka M, Iizumi Y, Watanabe M, Morita M, Nishimoto E, Taguchi T and Sakai T: The histone deacetylase inhibitor OBP-801 and eribulin synergistically inhibit the growth of triple-negative breast cancer cells with the suppression of survivin, Bcl-xL, and the MAPK pathway. *Breast Cancer Res Treat* 171: 43-52, 2018.
28. Ichijo H, Nishida E, Irie K, ten Dijke P, Saitoh M, Moriguchi T, Takagi M, Matsumoto K, Miyazono K and Gotoh Y: Induction of apoptosis by ASK1, a mammalian MAPKKK that activates SAPK/JNK and p38 signaling pathways. *Science* 275: 90-94, 1997.
29. Tai LM, Holloway KA, Male DK, Loughlin AJ and Romero IA: Amyloid-beta-induced occludin down-regulation and increased permeability in human brain endothelial cells is mediated by MAPK activation. *J Cell Mol Med* 14: 1101-1112, 2010.
30. Chen YY, Liu FC, Chou PY, Chien YC, Chang WS, Huang GJ, Wu CH and Sheu MJ: Ethanol extracts of fruiting bodies of *antrodia cinnamomea* suppress CL1-5 human lung adenocarcinoma cells migration by inhibiting matrix metalloproteinase-2/9 through ERK, JNK, p38, and PI3K/Akt signaling pathways. *Evid Based Complement Alternat Med* 2012: 378415, 2012.
31. Noguchi T, Takeda K, Matsuzawa A, Saegusa K, Nakano H, Gohda J, Inoue J and Ichijo H: Recruitment of tumor necrosis factor receptor-associated factor family proteins to apoptosis signal-regulating kinase 1 signalosome is essential for oxidative stress-induced cell death. *J Biol Chem* 280: 37033-37040, 2005.
32. Saxena G, Chen J and Shalev A: Intracellular shuttling and mitochondrial function of thioredoxin-interacting protein. *J Biol Chem* 285: 3997-4005, 2010.
33. Hatakeyama Y, Kobayashi K, Nagano T, Tamura D, Yamamoto M, Tachihara M, Kotani Y and Nishimura Y: Synergistic effects of pemetrexed and amrubicin in non-small cell lung cancer cell lines: Potential for combination therapy. *Cancer Lett* 343: 74-79, 2014.
34. Mok TS, Wu YL, Thongprasert S, Yang CH, Chu DT, Saijo N, Sunpaweravong P, Han B, Margono B, Ichinose Y, *et al*: Gefitinib or carboplatin-paclitaxel in pulmonary adenocarcinoma. *N Engl J Med* 361: 947-957, 2009.
35. Solomon BJ, Mok T, Kim DW, Wu YL, Nakagawa K, Mekhail T, Felip E, Cappuzzo F, Paolini J, Usari T, *et al*: First-line crizotinib versus chemotherapy in ALK-positive lung cancer. *N Engl J Med* 371: 2167-2177, 2014.
36. Brahmer J, Reckamp KL, Baas P, Crinò L, Eberhardt WE, Poddubska E, Antonia S, Pluzanski A, Vokes EE, Holgado E, *et al*: Nivolumab versus docetaxel in advanced squamous-cell non-small-cell lung cancer. *N Engl J Med* 373: 123-135, 2015.
37. Reck M, Rodríguez-Abreu D, Robinson AG, Hui R, Csósz T, Fülöp A, Gottfried M, Peled N, Tafreshi A, Cuffe S, *et al*: Pembrolizumab versus chemotherapy for PD-L1-positive non-small-cell lung cancer. *N Engl J Med* 375: 1823-1833, 2016.
38. Del Bufalo D, Desideri M, De Luca T, Di Martile M, Gabellini C, Monica V, Busso S, Eramo A, De Maria R, Milella M and Trisucchioglio D: Histone deacetylase inhibition synergistically enhances pemetrexed cytotoxicity through induction of apoptosis and autophagy in non-small cell lung cancer. *Mol Cancer* 13: 230, 2014.
39. Yu Y, Xing K, Badamas R, Kuszynski CA, Wu H and Lou MF: Overexpression of thioredoxin-binding protein 2 increases oxidation sensitivity and apoptosis in human lens epithelial cells. *Free Radic Biol Med* 57: 92-104, 2013.
40. Scherpereel A, Berghmans T, Lafitte JJ, Colinet B, Richez M, Bonduelle Y, Meert AP, Dhalluin X, Leclercq N, Paesmans M, *et al*: Valproate-doxorubicin: Promising therapy for progressing mesothelioma. A phase II study. *Eur Respir J* 37: 129-135, 2011.
41. Suzuki T, Minamide S, Iwasaki T, Yamamoto H and Kanda H: Cardiotoxicity of a new anthracycline derivative (SM-5887) following intravenous administration to rabbits: Comparative study with doxorubicin. *Invest New Drugs* 15: 219-225, 1997.
42. Noda T, Watanabe T, Kohda A, Hosokawa S and Suzuki T: Chronic effects of a novel synthetic anthracycline derivative (SM-5887) on normal heart and doxorubicin-induced cardiomyopathy in beagle dogs. *Invest New Drugs* 16: 121-128, 1998.